High–Yield Synthesis of Nickel and Nickel Phosphide Nanowires via Microwave–Assisted Processes

2 **AUTHORS**, INCLUDING:

Xianluo Hu

Huazhong University of Science and Techn…
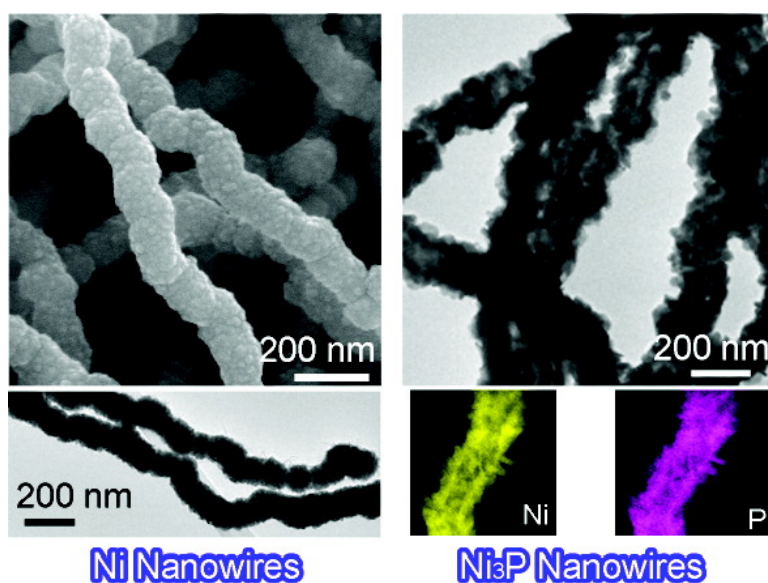
127 PUBLICATIONS **5,430** CITATIONS

SEE PROFILE

Article

High-Yield Synthesis of Nickel and Nickel Phosphide Nanowires via Microwave-Assisted Processes

Xianluo Hu, and Jimmy C. Yu

Ni Nanowires

Ni₃P Nanowires

More About This Article

Additional resources and features associated with this article are available within the HTML version:

- Supporting Information
- Access to high resolution figures
- Links to articles and content related to this article
- Copyright permission to reproduce figures and/or text from this article

View the Full Text HTML

High-Yield Synthesis of Nickel and Nickel Phosphide Nanowires via Microwave-Assisted Processes

Xianluo Hu*,[†,‡] and Jimmy C. Yu*,[‡]

Key Laboratory of Pesticide & Chemical Biology, Ministry of Education, College of Chemistry, Central China Normal University, Wuhan 430079, China, and Department of Chemistry and Center of Novel Functional Molecules, The Chinese University of Hong Kong, Shatin, New Territories, Hong Kong, China

A rapid and economical route based on an efficient microwave-assisted process has been developed to synthesize Ni nanowires in large quantities. The Ni nanostructures can be tuned by altering capping agents and solvents. Microwave-induced reaction of Ni with TOP can transform Ni nanowires into porous Ni_3P nanowires. The products were characterized by using X-ray diffraction (XRD), scanning electron microscopy (SEM), transmission electron microscopy (TEM), energy-dispersive X-ray (EDX) spectroscopy, elemental mapping, and magnetic characterization. This work presents an efficient and cost-effective approach that is potentially competitive for scaling-up industrial production. The as-formed Ni and Ni_3P nanowires not only provide flexible building blocks for advanced functional devices but also are ideal candidates for fundamental studies and potential magnetic, electronic, and catalytic applications.

Introduction

The past decade has witnessed significant growth in the field of one-dimensional (1D) nanomaterials because of their unique electrical, optical, and magnetic properties as well as their potential applications in mesoscopic device research.[1,2] In particular, 1D magnetic nanostructures are actively being explored because of their great potential as building blocks in magnetic recording, magnetic sensors, and spintronics applications.[3–12] Current preparation methods for 1D magnetic nanostructures are mainly based on template-assisted synthesis[13–15] and magnetic-field induced assembly of nanoparticles.[16] Those synthetic approaches usually give 1D magnetic nanostructures with low yields, poorly defined morphologies, low aspect ratios, and easy disassembly of nanoparticles. Mass and fast production of free-standing 1D magnetic nanowires of high quality still remains a significant challenge.

Herein we report a rapid and economical route based on an efficient microwave-assisted process for preparing to synthesize nickel (Ni) nanowires. It has been established that microwave irradiation is becoming an increasingly popular heating method for nanomaterials synthesis.[17–31] It offers a clean, cheap, and convenient strategy of heating that usually results in higher yields and shorter reaction time.[17–19] Modern microwave systems possess the capa-

* Corresponding author. E-mail: xlhu07@gmail.com; jimyu@cuhk.edu.hk.
† Central China Normal University.
‡ The Chinese University of Hong Kong.

(1) Xia, Y. N.; Yang, P. D.; Sun, Y. G.; Wu, Y. Y.; Mayers, B.; Gates, B.; Yin, Y. D.; Kim, F.; Yan, Y. Q. *Adv. Mater.* **2003,** *15,* 353.
(2) Huang, M. H.; Mao, S.; Feick, H.; Yan, H. Q.; Wu, Y. Y.; Kind, H.; Weber, E.; Russo, R.; Yang, P. D. *Science* **2001,** *292,* 1897.
(3) Whitney, T. M.; Jiang, J. S.; Searson, P. C.; Chien, C. L. *Science* **1993,** *261,* 1316.
(4) Mao, C. B.; Solis, D. J.; Reiss, B. D.; Kottmann, S. T.; Sweeney, R. Y.; Hayhurst, A.; Georgiou, G.; Iverson, B.; Belcher, A. M. *Science* **2004,** *303,* 213.
(5) Chueh, Y. L.; Lai, M. W.; Liang, J. Q.; Chou, L. J.; Wang, Z. L. *Adv. Funct. Mater.* **2006,** *16,* 2243.
(6) Song, R. Q.; Xu, A. W.; Yu, S. H. *J. Am. Chem. Soc.* **2007,** *129,* 4152.
(7) Liu, C. M.; Guo, L.; Wang, R. M.; Deng, Y.; Xu, H. B.; Yang, S. H. *Chem. Commun.* **2004,** 2726.
(8) Zhou, W.; Zheng, K.; He, L.; Wang, R. M.; Guo, L.; Chen, C. P.; Han, X.; Zhang, Z. *Nano Lett.* **2008,** *8,* 1147.
(9) Tanase, M.; Bauer, L. A.; Hultgren, A.; Silevitch, D. M.; Sun, L.; Reich, D. H.; Searson, P. C.; Meyer, G. J. *Nano Lett.* **2001,** *1,* 155.
(10) Morales, A. M.; Lieber, C. M. *Science* **1998,** *279,* 208.
(11) Zhang, Z. T.; Blom, D. A.; Gai, Z.; Thompson, J. R.; Shen, J.; Dai, S. *J. Am. Chem. Soc.* **2003,** *125,* 7528.
(12) Wu, H.; Zhang, R.; Liu, X. X.; Lin, D. D.; Pan, W. *Chem. Mater.* **2007,** *19,* 3506.
(13) Ersen, O.; Bégin, S.; Houllé, M.; Amadou, J.; Janowska, I.; Grenèche, J. M.; Crucifix, C.; Pham-Huu, C. *Nano Lett.* **2008,** *8,* 1033.
(14) Qin, J.; Nogues, J.; Mikhaylova, M.; Roig, A.; Munoz, J. S.; Muhammed, M. *Chem. Mater.* **2005,** *17,* 1829.
(15) Zhang, Z. T.; Rondinone, A. J.; Ma, J. X.; Shen, J.; Dai, S. *Adv. Mater.* **2005,** *17,* 1415.
(16) Jia, F. L.; Zhang, L. Z.; Shang, X. Y.; Yang, Y. *Adv. Mater.* **2008,** *20,* 1050.
(17) Komarneni, S. *Curr. Sci.* **2003,** *85,* 1730.
(18) Galema, S. A. *Chem. Soc. Rev.* **1997,** *26,* 233.
(19) Tsuji, M.; Hashimoto, M.; Nishizawa, Y.; Kubokawa, M.; Tsuji, T. *Chem. Eur. J.* **2005,** *11,* 440.
(20) Lu, Q. Y.; Gao, F.; Komarneni, S.; Mallouk, T. E. *J. Am. Chem. Soc.* **2004,** *126,* 8650.
(21) Makhluf, S.; Dror, R.; Nitzan, Y.; Abramovich, Y.; Jelinek, R.; Gedanken, A. *Adv. Funct. Mater.* **2005,** *15,* 1708.
(22) Zhu, Y. J.; Wang, W. W.; Qi, R. J.; Hu, X. L. *Angew. Chem., Int. Ed.* **2004,** *43,* 1410.
(23) Xu, L.; Ding, Y. S.; Chen, C. H.; Zhao, L. L.; Rimkus, C.; Joesten, R.; Suib, S. L. *Chem. Mater.* **2008,** *20,* 308.
(24) Panda, A. B.; Glaspell, G.; El-Shall, M. S. *J. Am. Soc. Chem.* **2006,** *128,* 2790.
(25) Celer, E. B.; Jaroniec, M. *J. Am. Chem. Soc.* **2006,** *128,* 14408.
(26) Hu, X. L.; Yu, J. C.; Gong, J. M.; Li, Q.; Li, G. S. *Adv. Mater.* **2007,** *19,* 2324.
(27) Hu, X. L.; Yu, J. C. *Adv. Funct. Mater.* **2008,** *18,* 880.
(28) Hu, X. L.; Yu, J. C. *J. Phys. Chem. C* **2007,** *111,* 11180.
(29) Yu, J. C.; Hu, X. L.; Li, Q.; Zhang, L. Z. *Chem. Commun.* **2005,** 2704.
(30) Yu, J. C.; Hu, X. L.; Li, Q.; Zheng, Z.; Xu, Y. M. *Chem.-Eur. J.* **2005,** *12,* 548.
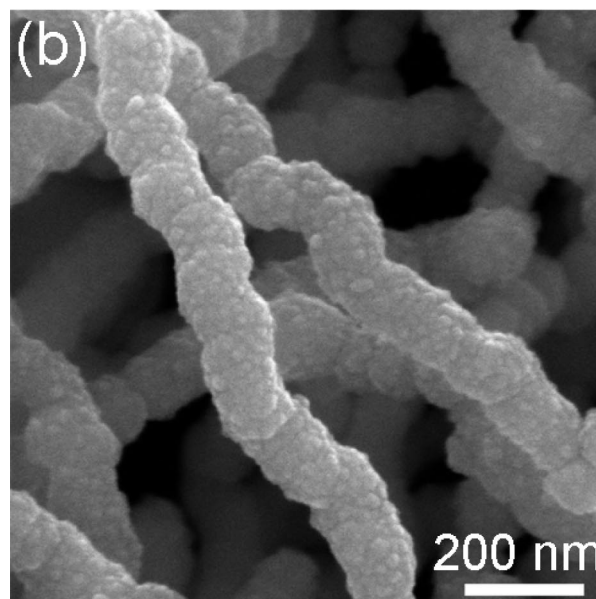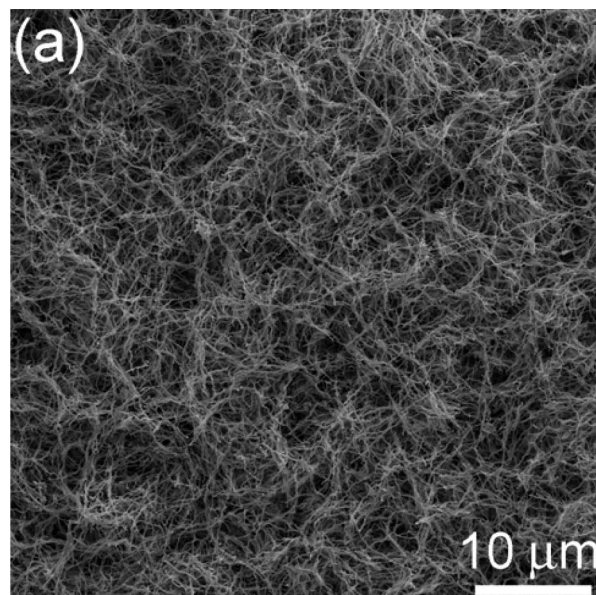(31) Hu, X. L.; Yu, J. C. *Chem.-Asian J.* **2006,** *1,* 605.

Table 1. Experimental Conditions for the Preparation of Ni Nanostructures[a]

sample no.	NiCl₂·6H₂O (mg)	solvent[b]	capping agent	temp (°C)	morphology[c]
S1	20	EG	TOPO (103 mg)	160	NWs
S2	10	EG	TOPO (103 mg)	160	NWs
S3	40	EG	TOPO (103 mg)	160	NWs + NPs
S4	60	EG	TOPO (103 mg)	160	NWs + NPs
S5	40	EG	TOPO (206 mg)	160	NFs
S6	20	EG	d	160	NFs
S7	20	DEG	TOPO (103 mg)	160	aggregated NRs
S8	20	DEG	TOPO (103 mg)	200	aggregated NPs
S9	20	BA	TOPO (103 mg)	160	e
S10	20	TEG	TOPO (103 mg)	160	e
S11	20	EG	PVP (103 mg)	160	NWs

[a] For each sample: amount of hydrazine monohydrate added = 165 μL; reaction time = 5 min. [b] The volume of solvent was 20 mL. [c] Nanowires, NWs; nanoparticles, NPs; nanorods, NRs; nanoflowers, NFs. [d] No capping agent was used. [e] No solid product was formed using BA and TEG as the solvent.
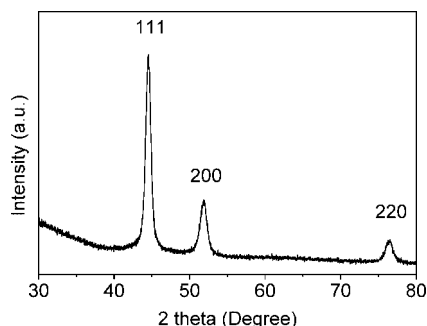
Figure 1. XRD pattern of sample S1.

bilities to program the duration and temperature. This allows one to fast screen a wide range of experimental parameters to enrich synthetic recipes and optimize material preparation.[17−31] Microwave heating is also unique in providing scale-up processes with a uniform reaction environment, thus paving the way to the large-scale industrial production of high-quality nanomaterials.[24−31] Although many magnetic nanoparticles have been successfully prepared by the microwave technique,[32,33] there is no report on solution-based anisotropic growth of magnetic in an alternating electromagnetic field of microwave irradiation, especially for structurally isotropic metals such as Ni with face-centered cubic (fcc) symmetry. We have recently developed the microwave-enhanced hydrothermal approaches for producing colloidal α-Fe₂O₃ nanocrystals with continuous aspect-ratio tuning and fine shape control,[26−28] carbon-based interconnected cable-like Ag/C,[29] spherical Se/C nanocomposites,[30] and superparamagnetic porous Fe₃O₄/C nanocomposites[31] in closed aqueous systems, by taking advantage of microwave irradiation and hydrothermal effects. In this work, we report that magnetic Ni nanowires can be synthesized in high yields in an open glycol system by microwave irradiation. The reaction proceeds within several minutes at atmospheric pressure without using any hard templates or catalysts. Therefore, our protocol is ideal for large-scale industrial production. Owing to the intrinsic anisotropic shape, these Ni nanowires exhibit enhanced mag-

(32) Komarneni, S.; D'Arrigo, M. C.; Leonelli, C.; Pellacani, G. C.; Katsuki, H. *J. Am. Ceram. Soc.* **1998**, *81*, 3041.
(33) Li, D.; Komarneni, S. *J. Am. Ceram. Soc.* **2006**, *89*, 1510.

Figure 2. (a) Low- and (b) high-magnification FE-SEM images of S1.

netic coercivity. Moreover, the as-prepared Ni nanowires serving as both the chemical precursor and the physical template can be easily converted into porous phosphide nanowires through a microwave-assisted route.
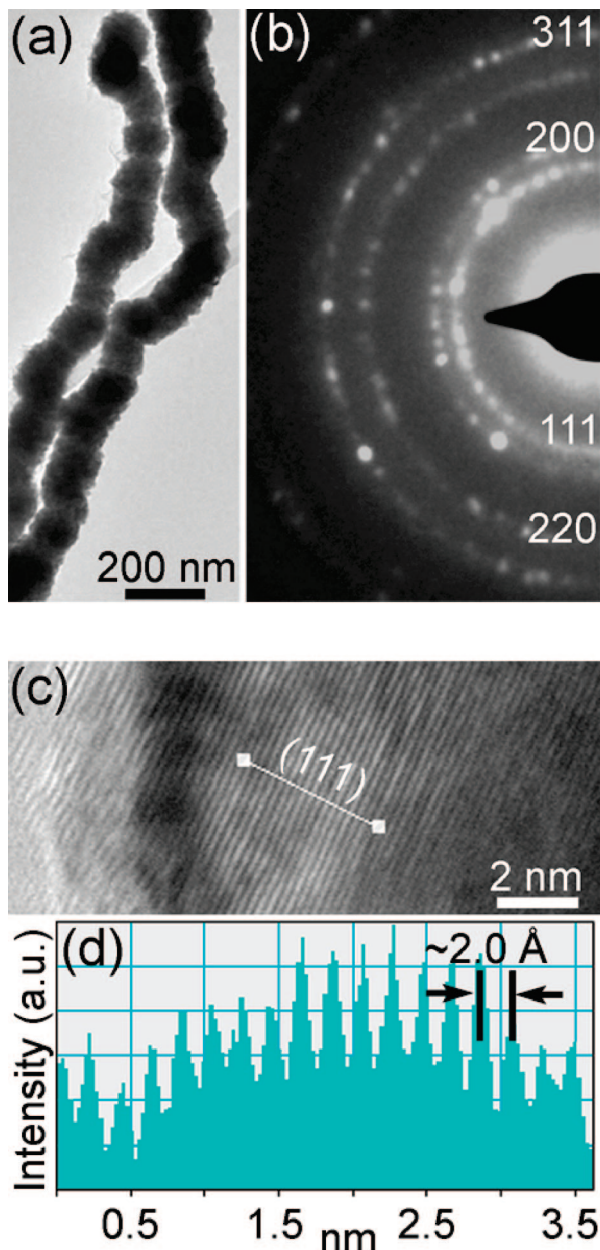
Experimental Section

Materials. All chemicals were used as received without further purification. NiCl₂·6H₂O (99.9%), ethylene glycol (EG, 99.8%), hydrazine monohydrate (98%), benzyl alcohol (BA, 99.8%), triethylene glycol (TEG, 99%), trioctylphosphine oxide (TOPO, 90%), and trioctylphosphine (TOP, 90%) were supplied by Aldrich. Poly(vinylpyrrolidone) (PVP, $M_w \approx 55\,000$) and diethylene glycol (DEG, 99%) were purchased from Sinopharm Chemical Reagent Co., Ltd., and International Laboratory (IL), respectively. Deionized water was used throughout.

Synthesis. All the samples were prepared in a microwave system (2.45 GHz, 300 W, Discover S-Class, CEM). The system was equipped with in situ magnetic stirring, and the glass reaction flask was fit with a water-cooled condenser. The exposure time and

Figure 3. (a) Bright-field TEM image of S1. (b) ED pattern indicating the polycrystalline nature of the nanowires. (c) Typical HRTEM image. (d) Corresponding intensity profile for the line scan across the lattice fringes.
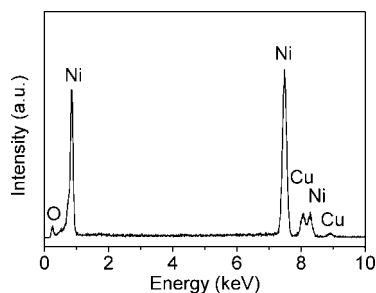
Figure 4. EDX spectrum of a single Ni nanowire from S1, where the signals of O and Cu are generated from the surface adsorption of TOPO and Cu grids, respectively.

temperature were programmed. The automatic temperature-control system allowed continuous monitoring and control (±1 °C) of the internal temperature of reaction systems. The preset profile (desired time and temperature) was followed automatically by continuously
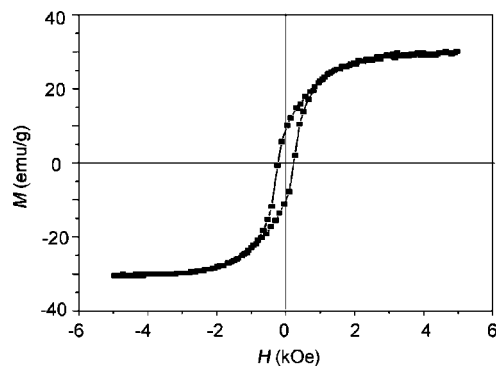
Figure 5. Hysteresis loop of S1 measured at 300 K.

Table 2. Magnetic Parameters of the Products

sample no.	saturation magnetization (M_s), emu g^{-1}	coercivity field (H_c), Oe
S1	30.1	239.3
S6	38.0	110.6
S8	33.3	167.9
S11	35.8	200.6

adjusting the applied microwave power. The detailed conditions for preparing some typical samples are listed in Table 1. In a typical procedure, NiCl₂·6H₂O (20 mg), TOPO (103 mg), and ethylene glycol (20 mL) were mixed in a 50-mL round-bottom flask. The mixture was vigorously stirred for 20 min, and then 165 µL of hydrazine monohydrate was added dropwise by an auto-pipette in 1 min. After treating the mixture at 160 °C for 5 min under microwave irradiation, it was cooled to room temperature. The product was collected, washed with deionized water and absolute ethanol, and dried in a vacuum at 60 °C for 4 h. A total of 10 mg of powder of the as-obtained Ni nanowires was added to 5 mL TOP solution. Then the mixture was treated under microwave irradiation at 265 °C for 5 min. After the mixture was cooled to room temperature, the product was collected, washed with deionized water and absolute ethanol, and dried in a vacuum at 60 °C for 4 h.

Characterization. The general morphology of the products was characterized by a field-emission scanning electron microscope (FE-SEM, FEI, Quanta 400 FEG). Transmission electron microscopy (TEM), high-resolution TEM (HRTEM), and high angle annular dark field scanning TEM (HAADF-STEM) measurements were carried out on a Tecnai F20 microscope (FEI, 200 kV) coupled with an HAADF detector and an energy-dispersive X-ray (EDX) spectrometer. Two-dimensional STEM-EDX elemental mapping was performed for the Ni₃P product. The electron probe size for the STEM-EDX analysis was about 1 nm. X-ray diffraction (XRD) patterns were collected using a Bruker D8 Advance diffractometer with high-intensity Cu Kα₁ irradiation (λ = 1.5406 Å). Powdered products were weighed out for magnetic characterization by vibrating sample magnetometry (VSM-7300, Lakeshore, U.S.A.).

Results and Discussion

Microwave-induced processing of a glycol NiCl₂·6H₂O solution in the presence of hydrazine and TOPO resulted in black powders in a high yield. XRD patterns provide crystallinity and phase information for the products. Figure 1 displays the typical XRD pattern for the sample S1. All the diffraction peaks in the pattern are readily indexed to a pure fcc crystal structure of Ni (*Fm3m*, JCPDS 87-0172, a = 3.5238 Å). No other impurities can be detected from this pattern. This indicates that well-crystallized Ni nanowires can be easily obtained under the current synthetic condition.
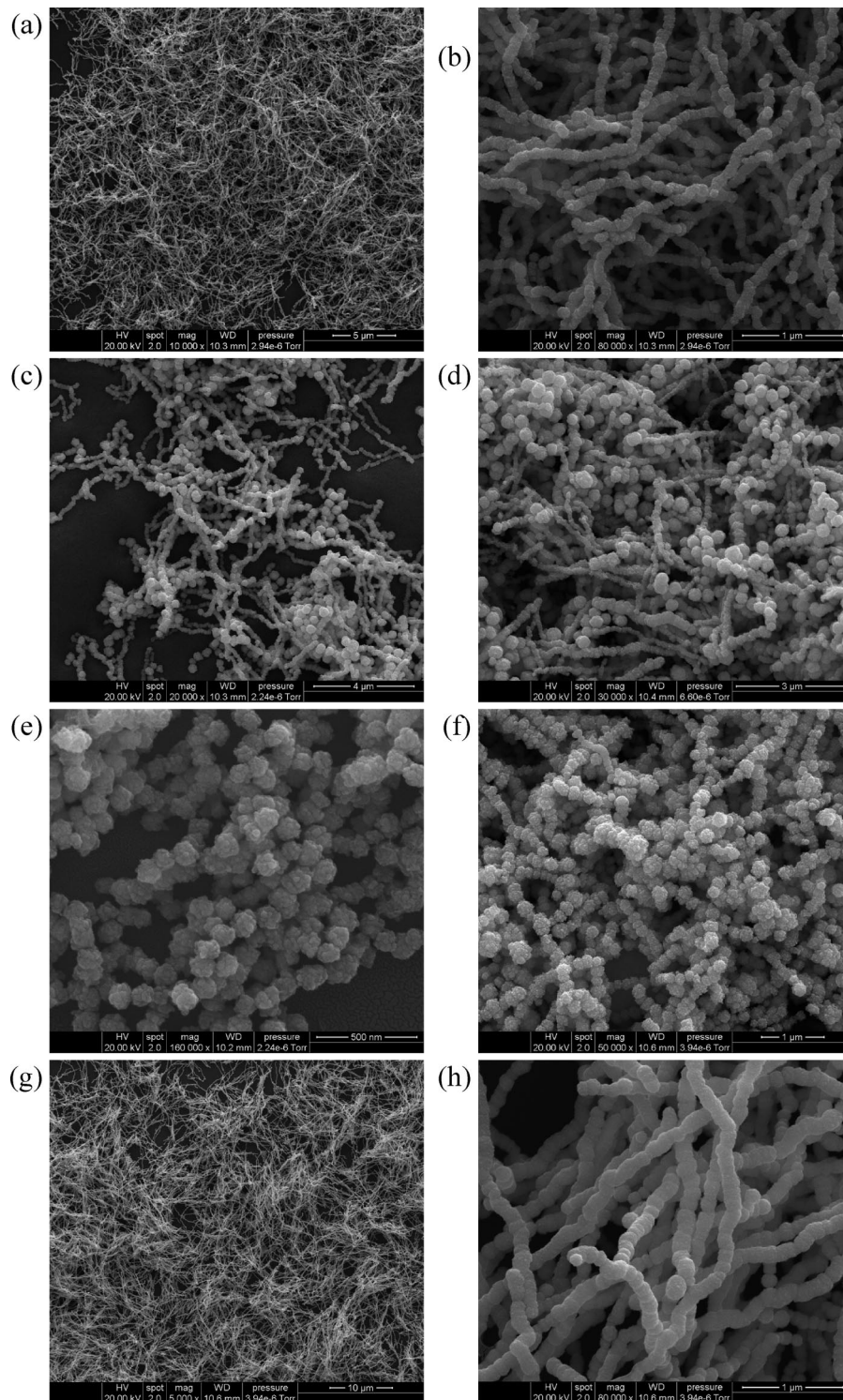
Figure 6. SEM images of the Ni products prepared in EG at different conditions: (a, b) S2, (c) S3, (d) S4, (e) S5, (f) S6, and (g, h) S11.

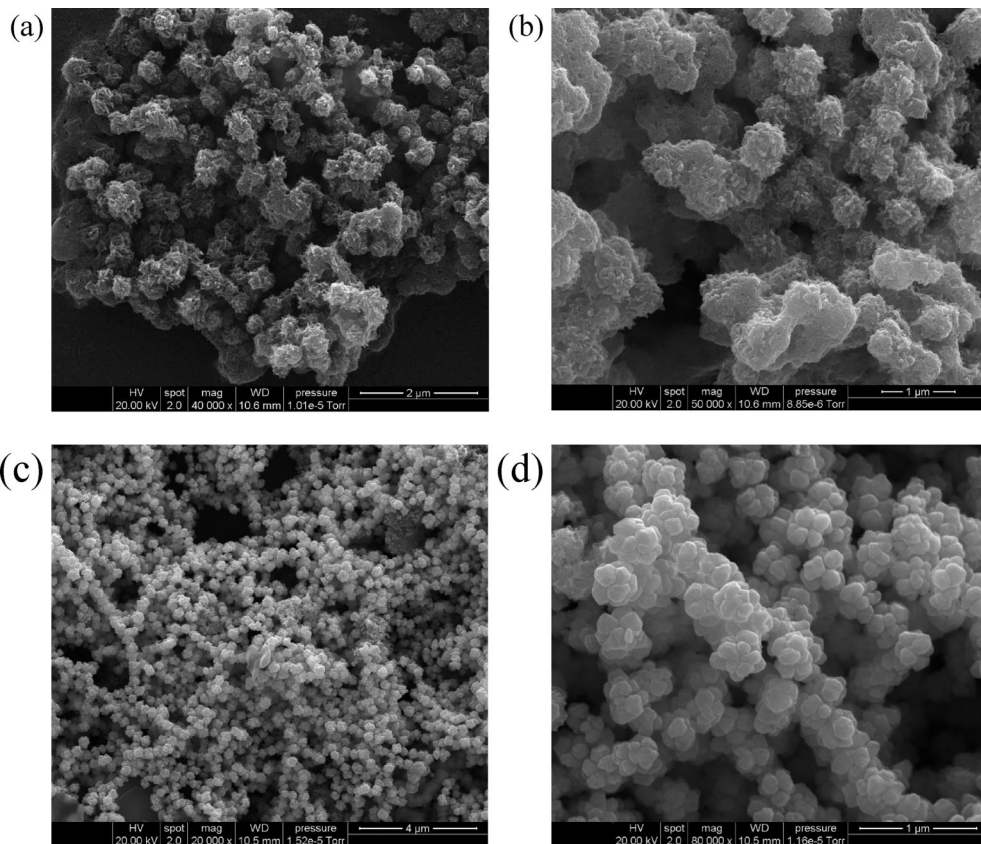**Scheme 1. Illustration of a Proposed Mechanism for the Formation of Ni Nanowires**
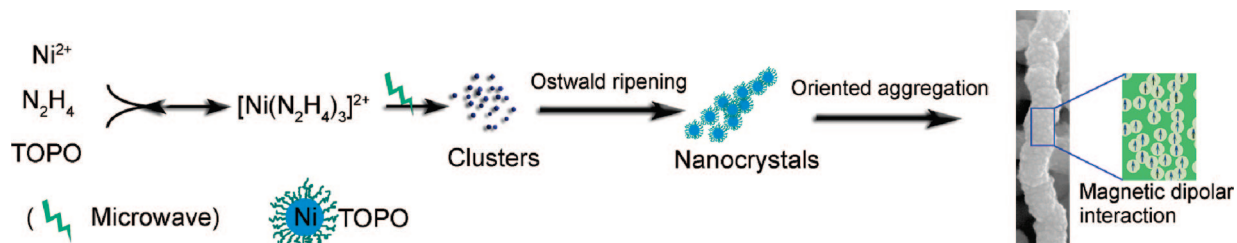
Figure 7. SEM images of the Ni products prepared in DEG: (a, b) S7 and (c, d) S8.
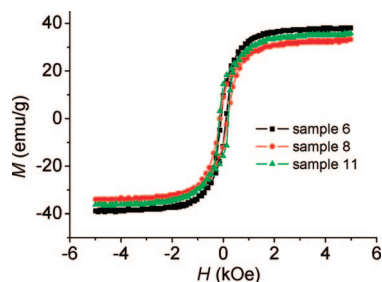

Figure 8. Magnetic hysteresis loops of S6, S8, and S10 measured at 300 K.

The size and shape of the products were examined by FE-SEM. Figure 2 shows the typical FE-SEM images for S1. The overall morphology of the product is shown in Figure 2a. It is observed that the product is composed of a large quantity of wire-like structures (nearly 100%) with high aspect ratios and lengths up to tens of micrometers. The aspect ratio is defined as the length of the major axis divided by the width of the minor axis. Thus, spherical particles have an aspect ratio of 1. Nanorods are defined as structures that have aspect ratios greater than 1 but less than 20; nanowires are analogous structures that have aspect ratios greater than 20.[34] Figure 2b shows the morphology of the product at a higher magnification, indicating these Ni nanowires with an average diameter of about 120 nm.

TEM and HRTEM images provide further insight into the microstructure of the product. Figure 3a displays the representative bright-field TEM image of S1, showing a well-defined wire morphology. The electron diffraction
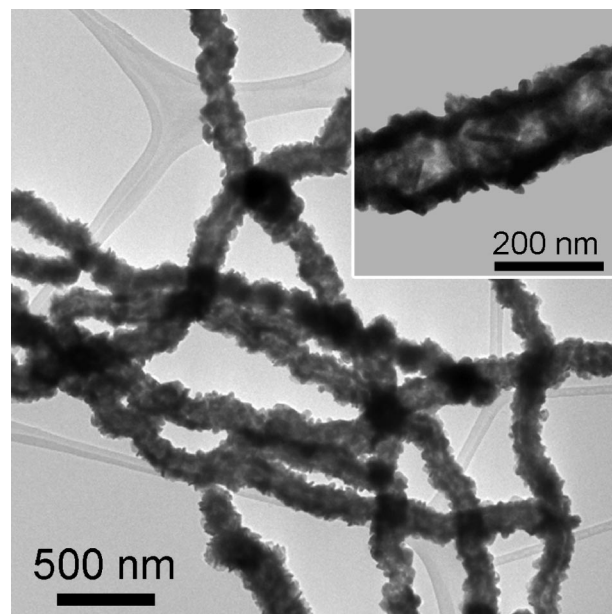

Figure 9. TEM image of the Ni₃P nanowires (inset: high-magnification TEM image showing the porous structure).

(ED) pattern (Figure 3b) was taken by focusing the electron beam on an individual nanowire, indicating the polycrystalline nature. Figure 3c shows a HRTEM image at the edge of an individual Ni nanowire. As shown in Figure 3d, a typical intensity profile covers the line scan (labeled by a line in Figure 3c) across the lattice fringes. The periodic fringe spacing of ∼2.0 Å agrees well with interplanar spacing between the {111} planes of the fcc Ni. The local elemental composition of the as-formed nanowires was studied by EDX microanalysis at the

(34) Murphy, C. J.; Jana, N. R. *Adv. Mater.* **2002**, *14*, 80.
(35) Liu, B.; Yu, S. H.; Li, L. J.; Zhang, Q.; Zhang, F.; Jiang, K. *Angew. Chem., Int. Ed.* **2004**, *43*, 4745.
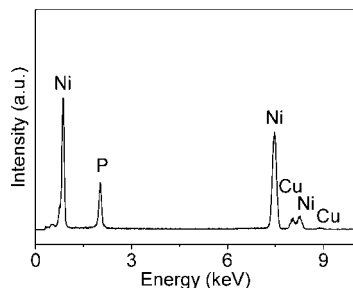
Figure 10. EDX spectrum of the as-prepared porous Ni_3P nanowires. The local elemental composition of the as-formed wires was studied by EDX microananlysis at the single-wire level. It confirms the presence of Ni and P. The signal of Cu is generated from the Cu grids.

single-nanowire level, shown in Figure 4. It confirms that the nanowires are composed of Ni.

The magnetic properties of the products were characterized by VSM. Figure 5 shows the room-temperature magnetization hysteresis loop for S1. Clearly, it reveals a typical ferromagnetic behavior with saturation magnetization (M_s) of 30.1 emu g^{-1} and coercivity field (H_c) of 239.3 Oe. The hysteresis curve is symmetric in shape with respect to zero magnetic field. This suggests that there is no exchange biasing effect which is usually induced by the presence of NiO.[16] It is worth noting that the Ni nanowires exhibit significantly enhanced magnetic coercivity (about 2 orders
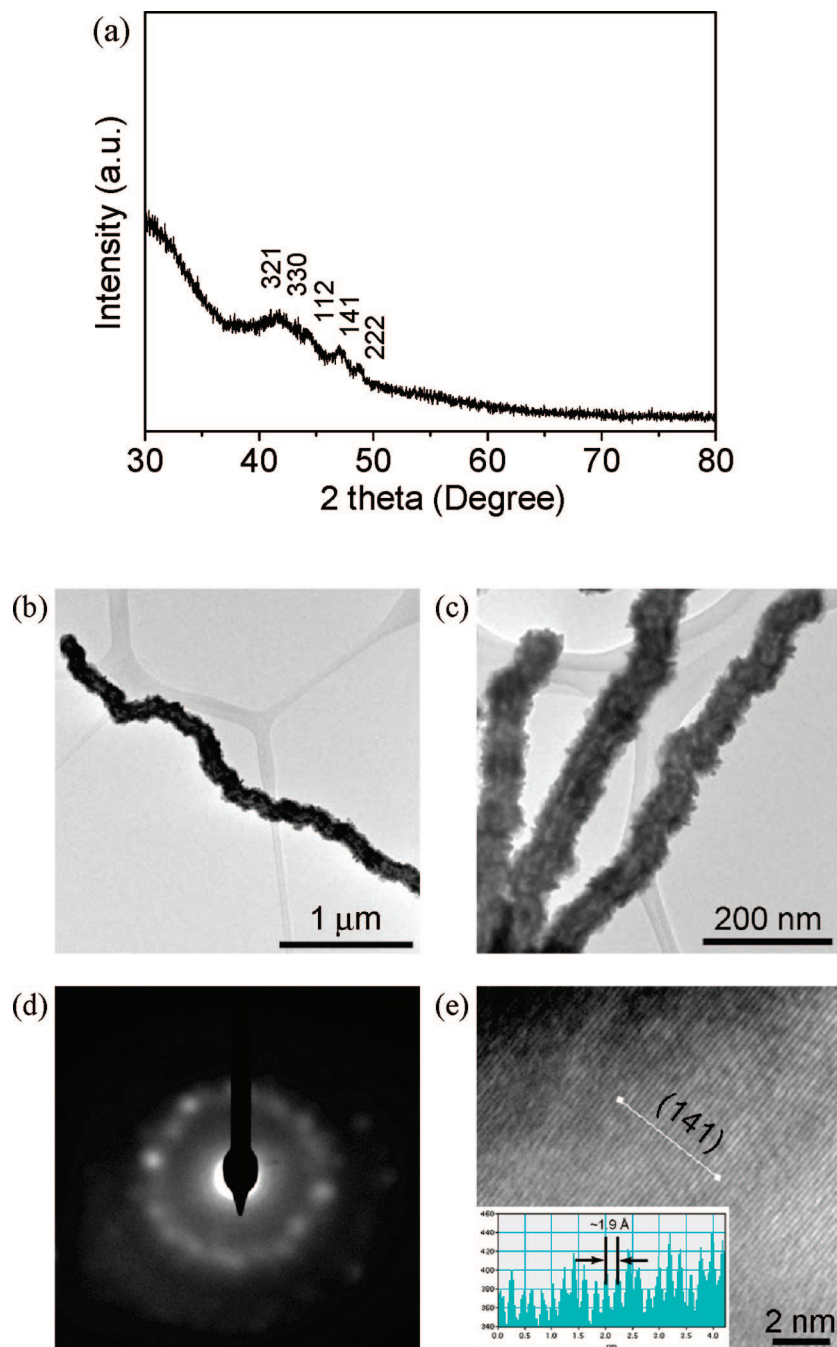
Figure 11. XRD pattern, TEM, and HRTEM images of porous Ni_3P nanowires: (a) XRD pattern. (b) A typical low-magnification TEM image showing the wire-like structure. (c) High-magnification TEM image. (d) ED pattern indicating the polycrystalline nature. (e) Typical HRTEM image taken from the edge of a wire. Inset: corresponding intensity profile for the line scan across the lattice fringes. The periodic fringe spacing of ~1.9 Å corresponds to interplanar spacing between the {141} planes of the bct Ni_3P.

High-Yield Synthesis of Ni and NiP₃ Nanowires

Chem. Mater., Vol. 20, No. 21, 2008 6749
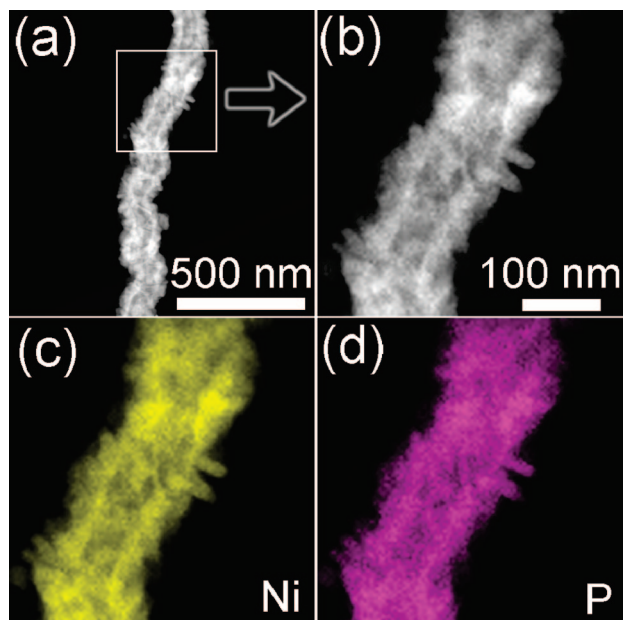
Figure 12. (a,b) HAADF-STEM and (c,d) elemental mapping images of a single Ni_3P nanowire.

of magnitude higher) compared with that of bulk Ni (0.7 Oe). This may be ascribed to the distinctive 1D anisotropic structure of the magnetic nanowires.

During the microwave-induced fabrication process, the introduction of capping agents promotes the anisotropic growth of Ni nanostructures, probably driven by the "oriented attachment" mechanism associate with Ostwald ripening.[34] Detailed studies reveal that capping agents, such as TOPO, play a key role in the formation of the nanowires. As displayed in Figures 2b and 3a, the wires are made up of small crystallites and have a rough surface. The crystallites attach to each other and grow into a wire due to the magnetic dipolar interaction of the Ni nanograins and the surface modification effect of TOPO. By reacting Ni^{2+} in a hydrazine solution, a dark blue complex of $[Ni(N_2H_4)_3]Cl_2$ is formed.[36] Under microwave irradiation, the excess hydrazine reduces the $[Ni(N_2H_4)_3]Cl_2$ complex into Ni nanocrystals.[37] Scheme 1 illustrates the general formation process of Ni nanowires. The products without adding TOPO only consist of spherical aggregates of Ni nanoparticles. We further investigated the effects of reactant concentration, solvents, and temperature on the morphology of the Ni products and also examined their magnetic proprieties. Results are summarized in Tables 1 and 2. Experimental results show that the morphologies and magnetic properties of Ni nanostructures are tunable as shown in Tables 1 and 2 and Figures 6−8.

Microwave irradiation also plays an important role in the formation of Ni nanowires. Owing to the excellent microwave-absorbing characteristics of polar glycol and metallic Ni, "hot spots" in the bulk solution and "hot surfaces" on metallic Ni can be created. They would speed up mass transfer and crystal growth. An added benefit of microwave irradiation is that it may induce localized ionic currents on the "hot surface" of Ni in an alternating electromagnetic field, providing additional driving force for directional crystallographic fusion of nuclei into nanowires. These unusual heating effects cannot be achieved by conventional means. In addition, dispersions of Ni nanowires in water or alcohol exhibit high stability under ultrasonic irradiation (Bransonic ultrasonic cleaner, model 3210EDTH, 47 kHz, 120 W, U.S.A.) even for 1 h with no notable morphological change.

We have further utilized the as-obtained Ni nanowires as a starting material to generate nanostructured nickel phosphide that has wide applications.[38,39] After microwave treating the Ni nanowires in liquid TOP at 265 °C for 5 min, nanowires with hierarchical pores are observed. The Ni nanowires serve as both chemical precursors and physical templates to form porous Ni_3P nanowires. Figure 9 shows the typical bright-field TEM image of the resulting porous nanowires. The inset of Figure 9 depicts a high-magnification TEM image for a part of an individual nanowire, indicating the presence of a large quantity of hierarchical pores. The hierarchical pores should benefit Ni_3P nanowires for the potential catalytic applications, providing much more efficient transport channels for the reactant molecules to get to the reactive sites of the Ni_3P framework. Compositional analysis of the porous nanowires by EDX indicates the presence of P and Ni (Figure 10). The average atomic ratio of P to Ni is about 1:2.96. Detailed XRD, ED, and HRTEM analyses (Figure 11) reveal that the porous nanowires are made of polycrystalline Ni_3P ($I\bar{4}$, JCPDS 74-1384; $a = 8.954$ Å, $c = 4.386$ Å). Figure 12a−d shows the typical high angle annular dark field scanning TEM (HAADF-STEM) and EDX elemental mapping images of an individual porous nanowire, further verifying the existence of P and Ni.

Conclusion

In conclusion, we have developed, for the first time, a fast and economical route based on an efficient microwave-assisted process for the preparation of Ni nanowires in large quantities. The Ni nanostructures can be tuned by altering capping agents and solvents. Also, microwave-induced transformation of Ni nanowires into porous Ni_3P nanowires can be easily realized, whereby the Ni nanowires serve as both chemical precursors and physical templates. The Ni and Ni_3P nanowires should be useful for fundamental studies and potential magnetic, electronic, and catalytic applications. It is important to note that our approach is highly efficient, taking less than 30 min to achieve gram-scale production. This route may also be extended to prepare other 1D metal and alloy magnetic nanostructures.

(36) Puntes, V. F.; Krishnan, K. M.; Alivisatos, A. P. *Science* **2001**, *291*, 2115.
(37) Wang, N.; Cao, X.; Kong, D. S.; Chen, W. M.; Guo, L.; Chen, C. P. *J. Phys. Chem. C* **2008**, *112*, 6613.
(38) Henkes, A. E.; Vasquez, Y.; Schaak, R. E. *J. Am. Chem. Soc.* **2007**, *129*, 1896.
(39) Park, J.; Koo, B.; Yoon, K. Y.; Hwang, Y.; Kang, M.; Park, J. G.; Hyeon, T. *J. Am. Chem. Soc.* **2005**, *127*, 8433.